Chondroitin-based nanoplexes as peptide delivery systems – investigations into the self-assembly process, solid-state and extended release characteristics

Anita Umerska[1)2)], Krzysztof Jan Paluch[3)], Maria Jose Santos-Martinez[1)4)], Carlos Medina[1)], Owen I. Corrigan[1)], Lidia Tajber[1)*]

1) School of Pharmacy and Pharmaceutical Sciences, Trinity College Dublin, Dublin 2, Ireland.
2) INSERM U1066, Micro et Nanomédecines Biomimétiques, Angers, France.
3) Bradford School of Pharmacy, Centre for Pharmaceutical Engineering Science, Faculty of Life Sciences, University of Bradford, Richmond Rd., BD71DP Bradford, W.Yorks., UK.
4) School of Medicine, Trinity College Dublin, Dublin 2, Ireland.

*To whom correspondence should be addressed: lidia.tajber@tcd.ie,
Phone: 00353 1 896 2787 Fax: 00353 1 896 2810

Abstract

A new type of self-assembled polyelectrolyte complex nanocarrier composed of chondroitin (CHON) and protamine (PROT) was designed and the ability of the carriers to bind salmon calcitonin (sCT) was examined. The response of sCT-loaded CHON/PROT NPs to a change in the properties of the liquid medium, e.g. its pH, composition or ionic strength was studied and *in vitro* peptide release assessed. The biocompatibility of the NPs was evaluated in Caco-2 cells. CHON/PROT NPs were successfully obtained with properties that were dependent on the concentration of the polyelectrolytes and their mixing ratio. X-ray diffraction determined the amorphous nature of the negatively charged NPs, while those with the positive surface potential were semi-crystalline. sCT was efficiently associated with the nanocarriers (98-100%) and a notably high drug loading (13-38%) was achieved. The particles had negative zeta potential values and were homogenously dispersed with sizes between 60 and 250 nm. CHON/PROT NPs released less than 10% of the total loaded peptide in the first hour of the *in vitro* release studies. The enthalpy of the decomposition exotherm correlated with the amount of sCT remaining in NPs after the release experiments. The composition of medium and its ionic strength were found to have a considerable influence on the release of sCT from CHON/PROT NPs. Complexation to CHON markedly reduced the toxic effects exerted by PROT and the NPs were compatible and well tolerated by Caco-2 cells.

KEYWORDS: chondroitin, protamine, calcitonin, nanoparticles, peptide delivery, polyelectrolyte complex, biocompatibility, toxicity, Caco-2 cells

List of abbreviations:

AB - acetate buffer

AE - association efficiency

ANOVA - one-way analysis of variance

Arg – arginine

ATR-FTIR - attenuated total reflectance Fourier transform infrared spectroscopy

CHON - chondroitin

COM1 - complex 1, composition: chondroitin/protamine mass mixing ratio=3.1, final chondroitin concentration=0.7 mg/ml

COM2 - complex 2, composition: chondroitin/protamine mass mixing ratio=3.1, final chondroitin concentration=1.4 mg/ml

COM3 - complex 3, composition: chondroitin/protamine mass mixing ratio=12.5, final chondroitin concentration=1.4 mg/ml

COM4 - complex 4, composition: chondroitin/protamine mass mixing ratio=3.1, final chondroitin concentration=2.1 mg/ml

COM5 - complex 5, composition: chondroitin/protamine mass mixing ratio=5, final chondroitin concentration=3.6 mg/ml

COM6 - complex 6, composition: chondroitin/protamine mass mixing ratio=0.2, final chondroitin concentration=0.16 mg/ml, positively charged nanoparticles

dH – enthalpy of process

DL - drug loading

DSC - differential scanning calorimetry

FBS - fetal bovine serum

HA - hyaluronic acid

HPLC – high performance liquid chromatography

kDa – kilodalton

kV – kilovolt

mA – milliampere

MEM - Eagle's Minimal Essential Medium

MMR - mass mixing ratio

MPS – mean particle size

MTS - 3-(4,5-dimethylthiazol-2-yl)-5-(3-carboxymethoxyphenyl)-2-(4-sulfophenyl)-2H-tetrazolium

MWCO – molecular weight cut-off

NP – nanoparticle

PBS - phosphate-buffered saline

PDI - polydispersity index

PROT – protamine

PXRD - powder X-ray diffraction

sCT - salmon calcitonin

Tg - glass transition

TR – transmittance

ZP - zeta potential

1. Introduction

Considerable efforts have been dedicated towards incorporation of bioactive ingredients into nanoparticles (NPs) composed of biodegradable polymers (Hamidi et al., 2008). There are a considerable number of polymers and techniques that are used to produce NPs, which allows a broad differentiation of their internal and external structures as well as composition and biological properties. The choice of the nanoparticle manufacturing method is influenced by the solubility of the active compound to be associated/complexed with the NPs as well as the solubility, chemical structure, characteristic chemical groups, molecular weight and crystallinity/amorphicity of the polymer (des Rieux et al., 2006). The most commonly used polymers are polyesters (e.g.

poly(lactic acid) and poly(lactic-co-glycolic acid)), either alone or in combination with other polymers (des Rieux et al., 2006). However, the limitation of biodegradable water-insoluble polymers is that they are mostly hydrophobic, whereas nucleic acids, many peptides and proteins, which are recognised to have a great potential in therapeutics, are hydrophilic. This leads to difficulties for the drug to be efficiently encapsulated (Sundar et al., 2010). Hence, the preparation of NPs with the employment of more hydrophilic and naturally occurring polymers has been explored. Among polymeric NPs, those composed of polyelectrolytes (polyelectrolyte complex NPs or nanoplexes) attract particular attention e.g. because of their water soluble character (Hartig et al., 2007). Amongst cationic polymers used in the formation of nanoplexes, undoubtedly chitosan is the most extensively investigated (Boateng et al., 2014). Recently, other polycations have also been employed in the formation of nanoplexes, e.g. polyarginine (Oyarzun-Ampuyero et al., 2011) and protamine (Umerska et al., 2014a). Protamine is a naturally occurring and strongly charged cationic protein already used in formulations containing insulin (AHFS Drug Information, 1989). Protamine (PROT) is rich in arginine and displays a membrane translocation activity (Reynolds et al., 2005). PROT offers a long history of use and established biological effects and safety in humans (Reynolds et al., 2005). It has been demonstrated to form polyelectrolyte complexes with oligonucleotides (Junghans et al., 2000; González Ferreiro et al., 2001) and glycosaminoglycans: hyaluronic acid (HA) (Umerska et al., 2014a) and heparin (Mori et al., 2010).

The recently described HA/PROT NPs have been shown to successfully encapsulate salmon calcitonin (sCT) with the association efficiency up to 100% and the advantage of high peptide loading (10-40% w/w) (Umerska et al., 2014a). However, the release of sCT was relatively quick as most of the peptide associated with the particles was released within 2-4 hours due to the weak electrostatic interactions between the species forming the NPs. Thus the strengthening of intermolecular interactions may decrease the release rate of sCT. Chondroitin sulphate (CHON) can be considered as a suitable candidate to form polyelectrolyte complexes with PROT and also

with sCT. CHON have weak (carboxylate) and strong (sulphate) acid residues, in contrast to HA, which only has carboxylate groups. Moreover, the charge density in CHON molecules is higher than in HA (Denuziere et al., 1996). Therefore it is anticipated that the electrostatic interactions between CHON and PROT as well as CHON and a cationic sCT will be stronger compared to HA-based interactions. Due to its acidic nature CHON is able to produce ionic complexes with positively charged molecules. Indeed, similarly to HA, CHON has been shown to form polyelectrolyte complexes with chitosan (Denuziere et al., 1996, Place et al., 2014), trimethylchitosan (Place et al., 2014), lysozyme (van Damme et al., 1994) and polyethylenimine (Pathak et al., 2009).

CHON is an abundant glycosaminoglycan found in cartilage, bone and connective mammalian tissue. It exhibits a wide variety of biological functions and is currently used as an anti-inflammatory, chondroprotective and antirheumatic drug. CHON has been shown to be absorbed after oral administration in humans as a high molecular weight polysaccharide (Volpi, 2002). sCT, currently recommended for short term use in Paget's disease, acute bone loss due to sudden immobilisation and hypercalcaemia caused by cancer (EMA, 2014), has also been considered as a promising candidate to be used in osteoarthritis (Manicourt et al., 2005) and in combined therapy with alendronate in patients with rheumatoid arthritis (Ozoran et al., 2007). The biological and pharmacological properties of sCT are therefore complementary to those of CHON.

A combination of CHON with its anti-inflammatory and chondroprotective action and PROT, due to its membrane-translocating activity, may be interesting from the therapeutic point of view and such hybrid CHON/PROT NPs may have the potential to form carriers for the oral delivery of peptides, in particular sCT. Patient compliance was identified as one of the major issues of long-term therapies involving parenteral administration of peptides, hence developing such a delivery system is of significance (Lee and Sinko, 2000). The low bioavailability of sCT after oral administration has been attributed to proteolytic enzymatic degradation and low intrinsic intestinal membrane permeability (Lee and Sinko, 2000), however a correlation between enhancement of

143 sCT absorption and mucoadhesion in rats was found by Sakuma et al. (1999, 2002). The
144 Sakuma's delivery system comprised NPs with hydrophilic, ionic polymeric chains attached to the
145 NP surface and sCT incorporated in the NPs non-covalently. These NPs also protected the
146 peptide against digestive enzymatic degradation *in vitro* and shielding sCT from pepsin and
147 trypsin was also observed for polymeric HA/PROT NPs (Umerska et al., 2014a).
148 Considering the above and that no drug delivery system, especially in the nanoparticulate format,
149 comprising CHON and PROT has been reported to date, the aims of the current work were to
150 investigate the conditions of such carrier formation by adopting the previously presented
151 manufacturing process (Umerska et al., 2012; Umerska et al., 2014a, Umerska et al., 2014b), to
152 evaluate the conditions of NP formation and their properties as well as to explore the ability of
153 CHON/PROT NPs to bind and release sCT. Bearing in mind that CHON/PROT NPs are
154 polyelectrolyte complex NPs, their potential as extended/controlled drug release systems was
155 also studied and evaluation of suitability of solid-state techniques, as methods supporting the
156 peptide release studies, was performed.

157 **2 Materials and methods**

158 **2.1 Materials**

159 Chondroitin 4-sulfate sodium salt (CHON) and protamine sulphate (PROT, molecular weight of
160 5.1 kDa; manufacturer's data) were purchased from Sigma (Ireland). Salmon calcitonin (sCT,
161 molecular weight 3.4 kDa, freely soluble in water, isoelectric point of 8.86 (Torres-Lugo and
162 Peppas, 1999) and net charge at pH 7.4 of approximately 3+) was obtained from PolyPeptide
163 Laboratories (Denmark). CellTiter 96® Non-Radioactive Cell Proliferation Assay was obtained
164 from Promega Corporation (USA). Other cell culture reagents were provided by Sigma Aldrich
165 (Ireland). All other reagents, chemicals and solvents were of analytical grade.
166 The molecular weight of CHON was determined using a gel permeation chromatography system
167 previously described (Umerska et al., 2012). Briefly, CHON was dissolved in a mobile phase
168 composed of 0.2M NaCl and 0.01M NaH_2PO_4 brought to pH 7.4 with NaOH solution. Pullulan

standards (PL Polymer Laboratoires, Germany) were used to construct the calibration curve. Standards and samples were prepared as 1 mg/ml solutions in the mobile phase. 100 µl of the standard or sample was injected into the Plaquagel-OH mixed 8µm 300 × 7.5 mm column (Polymer Laboratories Ltd., UK) using a flow rate of 1 ml/min. A Waters 410 refractive index detector was employed. Data collection and integration were accomplished using CLASS-VP software (version 6.10) with GPC for Class VP (version 1.02) (Shimadzu, Japan). The weight average molecular weight (Mw) of CHON was 58.6±0.23 kDa.

2.2 Preparation of CHON/PROT carriers and CHON/PROT/sCT NPs

The CHON solutions with concentrations of 1, 2, 3 or 5 mg/ml as well as the PROT solutions with concentrations of 0.4-12 mg/ml were prepared in deionised water. NP carriers (NPs without the cargo) were formed by adding 4 ml of an aqueous PROT solution to 10 ml of a CHON solution at room temperature under magnetic stirring. The stirring was maintained for 10 minutes to allow stabilisation of the system. A dispersion of particles was instantaneously obtained upon mixing of the polymer solutions. As a range of CHON/PROT ratios were used, the NP dispersions that were formed had different compositions of CHON (equivalent to 0.71 mg/ml, 1.43 mg/ml 2.14 mg/ml or 3.57 mg/ml in the final formulation) and PROT (equivalent to 0.11-3.43 mg/ml in the final formulation).

NPs containing sCT were formed following the above procedure. An appropriate quantity of the peptide, resulting in the final sCT concentration in the NP dispersion of 0.5 and 1.0 mg/ml, was dissolved in the CHON solution prior to mixing with the PROT solution.

2.3 NPs characterisation and stability

2.3.1 Transmittance measurements

The transmittance of the NP dispersions was measured using an UV-1700 PharmaSpec UV-Visible spectrophotometer (Shimadzu) at an operating wavelength of 500 nm in optically homogenous quartz cuvettes (Hellma, Germany) with a light path of 10 mm (Umerska et al., 2012).

195 **2.3.2. Dynamic viscosity and quantification of associated in NPs CHON**

196 Dynamic viscosity measurements of CHON and PROT solutions as well as NP dispersions were
197 carried out with an SV-10 Vibro Viscometer (A&D Company Limited) at 25±0.2 ºC. The instrument
198 was calibrated using deionised water before measurements and the analysis was done at least
199 in triplicate for each batch of the liquid sample. The amount of free/unassociated with NPs CHON
200 was determined from viscosity measurements of continuous phases of NP dispersions. The
201 viscosity value of pure CHON solution, for a given polymer concentration, was taken as containing
202 100% free CHON, while the viscosity of water was taken as containing 0% free CHON, since the
203 viscosity of the continuous phase of a colloidal dispersion compared to that of water can be
204 correlated with the quantity of free polymer present in the liquid (Umerska et al., 2012). The
205 amount bound/associated in NPs CHON (expressed as %) was calculated as a difference
206 between the starting quantity of CHON used in formulation (using the initial CHON concentration)
207 and the quantity of free/unassociated CHON.

208 **2.3.3 Particle size and zeta potential analysis**

209 The intensity-averaged mean particle size (hydrodynamic particle diameter), polydispersity index
210 (PDI) and zeta potential (ZP) values of the NPs were determined as previously described by
211 Umerska et al., (2014b). Samples, in their native dispersions, were placed into folded capillary
212 cells without dilution. Each analysis was carried out at 25 ºC with the equilibration time set to 5
213 minutes. The readings were repeated at least three times for each batch and the average values
214 of at least three batches are presented. The results obtained were corrected for the sample
215 viscosity measured at described above.

216 **2.4 Salmon calcitonin (sCT) loading studies**

217 **2.4.1 Separation of non-associated sCT**

218 Non-associated sCT was separated from the NPs using a combined ultrafiltration-centrifugation
219 technique (Amicon® Ultra-15, MWCO of 30 kDa, Millipore, USA). A total of 5 ml of sample was
220 placed in the sample reservoir (donor phase) of the centrifugal filter device and centrifuged for 1

hour at 3,000 rpm (4,537 g). After centrifugation, the volume of the solution in the filtrate vial (acceptor phase) was measured, and the filtrate was assayed for sCT content via high performance liquid chromatography (HPLC), as described below. This quantity of sCT was referred to as the non-associated sCT.

The NP suspension from the sample reservoir was standardized to 5 ml with deionised water. A total of 0.75 ml of the NP suspension from the sample reservoir was mixed with 0.75 ml of 0.1 mM NaOH (this NaOH concentration was optimised and did not cause sCT degradation) to break up the NPs and release sCT, and the mixture was centrifuged for 30 minutes at 13,000 rpm (16,060 g). The supernatant was assayed for sCT content via HPLC, and this portion of the peptide was referred to as the extracted sCT. The remainder of the dispersion from the sample reservoir was analysed for particle size, zeta potential and transmittance. The particle size, zeta potential, transmittance, pH and viscosity of NPs before separation of the non-associated sCT were also measured.

The association efficiency (AE) and drug loading (DL) were calculated using the following equations (Umerska et al., 2014b):

$$AE = \left[\frac{A-B}{A}\right] * 100\% \qquad \text{(Eqn. 1)}$$

where A is the total amount (mass) of the sCT, and B is the mass of the non-associated sCT

$$DL = \left[\frac{A-B}{C}\right] * 100\% \qquad \text{(Eqn. 2)}$$

where C is the total weight of all components of the NPs (the associated sCT and the mass of CHON and PROT used for the preparation of NPs).

2.4.2 Colloidal behaviour of CHON/PROT/sCT NPs in different media

Aliquots of 250 µl of sCT-loaded CHON/PROT NPs (CHON conc. 2.1 mg/ml, sCT conc. 1 mg/ml, CHON/PROT mass mixing ratio (MMR)=6.3) were added to 2.25 ml of the dispersant. The following dispersants were used:

- phosphate-buffered saline (PBS) pH=7.4 (137 mM NaCl, 2.7 mM KCl, 1.4 mM NaH_2PO_4,

246 1.3 mM Na_2HPO_4 adjusted to pH 7.4 with NaOH solution),

247 - PBS pH=5 (137 mM NaCl, 2.7 mM KCl, 1.4 mM NaH_2PO_4, 1.3 mM Na_2HPO_4 adjusted to
248 pH 5 with HCl solution),
249 - diluted PBS pH=7.4 (1:10 dilution with deionised water of pH 7.4 PBS),
250 - acetate buffer pH=5 (0.0375M CH_3COOH and 0.0643M of CH_3COONa pH=5),
251 - acetate buffer pH=7.4 (0.0375M CH_3COOH and 0.0643M of CH_3COONa adjusted to pH
252 7.4 with NaOH solution),
253 - diluted acetate buffer pH=5 (1:10 dilution with deionised water of pH 5 acetate buffer),
254 - deionised water
255 - HCl 0.07M pH=1.2
256 - Eagle's Minimal Essential Medium (MEM), pH=7.4
257 - aqueous NaCl solution with the following concentrations: 0.09%, 0.23%, 0.45%, 0.9% and
258 1.8% w/v

259 Samples were incubated at 37 ºC at 100 rpm in a reciprocal shaking water bath (model 25,
260 Precision Scientific, India). Size and zeta potential measurements (Section 2.3.2) were performed
261 after 1 hour of incubation.

262 **2.4.3 Release studies**

263 Aliquots of 250 µl of sCT-loaded CHON/PROT NPs (CHON conc. 2.1 mg/ml, sCT conc. 1 mg/ml,
264 CHON/PROT mass mixing ratio=6.3) were added to 2.25 ml of dispersant. The following
265 dispersants were used: PBS (pH 5 and 7.4), diluted PBS (pH 7.4), acetate buffer (pH 5 and 7.4),
266 diluted acetate buffer (pH 5), deionised water and 0.07M HCl (pH 1.2). The samples were
267 incubated at 37 ºC at 100 rpm in a reciprocal shaking water bath (model 25, Precision Scientific,
268 India). After 1, 2, 4, 6 and 24 hours, 2.5 ml aliquots were withdrawn, and the released sCT was
269 separated using the combined ultrafiltration-centrifugation technique as described above. The
270 samples were centrifuged at 4,500 rpm (6,805 g) for 15 minutes. After centrifugation, the volume

of the solution from the filtrate vial (acceptor phase) was measured, and the filtrate was assayed for sCT content by HPLC (released sCT; the HPLC method is described below). The NP dispersion from the sample reservoir was made up to 2.5 ml with the dispersant and returned to the water bath to continue the release studies.

The data from the release studies were fitted to the first-order equation:

$$W = W_{\infty}(1 - e^{-kt}) \qquad \text{(Eqn. 3)}$$

where W is the amount of the peptide released at time t (based on cumulative release), W_{∞} is the amount of the peptide released at infinity and k is the release rate constant (Corrigan et al., 2006).

2.4.4 Quantification of sCT

Analysis of sCT content was performed using an HPLC system as described previously (Umerska et al., 2014b). Briefly, standard solutions of sCT (1.5–50 µg/ml) were prepared in deionised water, and 50 µl of the standard or sample was injected into the Jones Chromatography Genesis 4µ C18 150x4.6 mm column. A flow rate of 1 ml/min was employed using a mobile phase composed of 0.116% w/v NaCl, 0.032% v/v trifluoroacetic acid and 34% v/v acetonitrile. The UV detection was carried out at 215 nm. The sCT peak had a retention time of ~5 min. Data collection and integration were accomplished using CLASS-VP software (version 6.10, Shimadzu, Japan).

2.5 Solid state characterisation

Solutions of CHON (5 mg/ml) and PROT (12 mg/ml) as well as a range of CHON/PROT NP dispersions (without sCT) were prepared as described in Section 2.2. The following CHON/PROT MMRs and CHON concentrations were tested: complex 1 (COM1, MMR=3.1, final CHON conc.=0.7 mg/ml), complex 2 (COM2, MMR=3.1, final CHON conc.=1.4 mg/ml), complex 3 (COM3, MMR=12.5, final CHON conc.=1.4 mg/ml), complex 4 (COM4, MMR=3.1, final CHON conc.=2.1 mg/ml), complex 5 (COM5, MMR=5, final CHON conc.=3.6 mg/ml) and complex 6 (COM6, MMR=0.2, final CHON conc.=0.16 mg/ml). In addition, samples of CHON/PROT/sCT NPs were collected after 6h of release studies (release studies are described in Section 2.4.3).

All liquid samples were freeze dried following the procedure presented by Umerska et al. (2012)

297 and analysed by powder X-ray diffraction (PXRD), differential scanning calorimetry (DSC) and
298 attenuated total reflectance Fourier transform infrared spectroscopy (ATR-FTIR) (Paluch et al.,
299 2010, 2013). Briefly, a Miniflex II Desktop X-ray diffractometer Rigaku with a Haskris cooling unit
300 was employed. The tube output voltage used was 30 kV and tube output current was 15 mA. A
301 Cu-tube with Ni-filter suppressing Kβ radiation was used. Measurements were taken from 5 to 40
302 on the 2 theta scale at a step size of 0.05° per second. DSC experiments were performed using
303 a Mettler Toledo DSC 821e with a refrigerated cooling system LabPlant RP-100. Nitrogen was
304 used as the purge gas. Aluminium sample holders were sealed with a lid and pierced to provide
305 three vent holes. Sample weights were approximately 3 mg and measurements were carried out
306 at a heating rate of 10 °C/min. The unit was calibrated with indium and zinc standards. ATR-FTIR
307 spectra were recorded on a PerkinElmer Spectrum 1 IR Spectrometer and evaluated using
308 Spectrum v5.0.1 software. The spectral range was 650–4000 cm^{-1} and a resolution of 4 cm^{-1}. Six
309 scans were collected, averaged and normalised to obtain good quality spectra.

310 **2.6 Cell culture and *in vitro* cytotoxicity studies**

311 Intestinal epithelial cells (Caco-2) were obtained from the European Collection of Cell Cultures.
312 Cells were cultured as a monolayer in Eagle's Minimal Essential Medium (MEM) supplemented
313 with 20% fetal bovine serum (FBS), penicillin (0.006 mg/ml), streptomycin (0.01 mg/ml),
314 gentamicin (0.005 mg/ml), sodium bicarbonate (2.2 g/l) and sodium pyruvate (0.11 g/l) in a 5%
315 CO_2 and 37 ºC humidified atmosphere (CO_2 incubator series 8000DH, ThermoScientific, USA).
316 Cells were supplied with fresh medium every second day and split after detachment with EDTA-
317 trypsin twice a week. The passage number range was maintained between 20 and 30.

318 **2.6.1 MTS assay**

319 The Caco-2 cells were seeded into flat-bottom 96-well plates in 100 µl of MEM containing 20% of
320 FBS at a density of 25,000 cells per well and incubated at 37 ºC for 24 hours. The medium was
321 replaced with 100 µl of the sample dispersed or dissolved in serum-free media. After 72 hours of
322 incubation, the supernatant was removed from the wells and replaced with serum-free media. An

amount of 20 µl of MTS reagent prepared according to the manufacturer protocol was added into each well; in the case of the positive control (0% viability), the media was replaced with a 10% SDS solution in serum-free media 30 min before the addition of MTS reagent. After 4 hours, the UV absorbance of the formazan product was measured spectrophotometrically (FLUOstar Optima microplate reader, BMG Labtech) at 492 nm. The positive control was treated as a blank, and its absorbance was subtracted from each reading. The cell viability was expressed as the ratio of the absorbance reading of the cells treated with different samples and that of the negative control (cells treated with serum-free MEM), which was assumed to have 100% of cell viability. Experiments were repeated 3 times.

2.7 Statistical analysis

The statistical significance of the differences between samples from *in vitro* release studies was determined using one-way analysis of variance (ANOVA) followed by the post-hoc Tukey's test using Minitab software. Differences were considered significant at $p<0.05$. As regards cell culture studies, statistical differences between groups were determined by Student's t-test. A two-tailed p-value <0.05 was considered as statistically significant.

3. Results

3.1 CHON/PROT NPs: formation and formulation variables

Depending on CHON/PROT mass mixing ratio (MMR) and the concentration of both polyelectrolytes, different types of CHON/PROT dispersions, i.e. solution (transmittance above 95%), opalescent (transmittance 85-95%), turbid (transmittance 0.1-85%) dispersion or a phase separation were observed. Fig. 1 shows the properties of macroscopically homogeneous (i.e. either having the appearance of a solution or being opalescent or turbid) CHON/PROT polyelectrolyte complexes dispersed in the form of colloidal particles.

For each concentration of CHON tested the systems containing more PROT (lower CHON/PROT MMRs) were generally more turbid (Fig. 1A). All dispersions that are included in Fig.1 were visually homogenous. The phase separation (observed as particle flocculation) occurred at

CHON/PROT MMRs of 1.0, 1.1, 1.0 and 1.1 for CHON concentrations of 0.7, 1.4, 2.1 and 3.6 mg/ml, respectively.

Fig.1B shows the mean hydrodynamic diameter of CHON/PROT NPs. CHON/PROT NPs had the size ranging from 78±3 or 78±12 nm (CHON of 1.4 mg/ml, CHON/PROT MMR=3.0 and CHON of 0.7 mg/ml, CHON/PROT MMR=3.2, respectively) to 296±16 nm (CHON of 3.6 mg/ml, CHON/PROT MMR=1.2). The particle size increased with an increasing amount of PROT in the formulation (decreasing CHON/PROT MMR). The concentration of CHON was also found to affect the particle size of CHON/PROT NPs, especially when it increased from 1.4 mg/ml to 2.1 mg/ml.

Fig. 1C presents PDI of CHON/PROT NPs. The PDI values varied from 0.11±0.00 (CHON of 1.4 mg/ml and CHON/PROT MMR=1.4) to 0.43±0.02 (CHON of 3.6 mg/ml and CHON/PROT MMR=10.6). The CHON/PROT MMR had a considerable influence on the size distribution of NPs. The higher the amount of PROT in the dispersion (i.e. the lower CHON/PROT MMR), the more homogenous the size distribution of the particles was. Also, the PDI values generally increased with the increasing concentration of CHON and decreased with an increase in the particle size.

All physically stable (i.e. non-sedimenting and non-aggregating) dispersions were characterised by a negative surface charge between -27.6±5.99 mV (CHON of 2.1 mg/ml, CHON/PROT MMR= 1.2) and -63.1±8.59 mV (CHON of 3.6 mg/ml, CHON/PROT MMR=10.6) (Fig. 1D). The surface charge of CHON/PROT NPs decreased as the CHON/PROT MMR decreased. This decrease was marginal at high MMRs (approximately 2-20) and more significant at lower MMRs (approximately 1.2-2).

The efforts to obtain physically stable (for at least 24h) positively charged CHON/PROT dispersions of NPs were unsuccessful. When CHON solution (0.16 mg/ml) was mixed with PROT solution (0.7 mg/ml) at CHON/PROT MMR of 0.2, a very homogenously dispersed (PDI of 0.014± 0.010) small (211±6 nm) NPs bearing positive surface charge of 11.6±0.78 mV were obtained (Fig. 1b, c and d). Aggregation of the positively charged NPs forming larger NPs and later

375 microparticles was observed after a few hours of storing the dispersion at room temperature (Fig.
376 2).

377 **3.2 Formation and characterisation of sCT-loaded CHON/PROT NPs**

378 The success of loading of sCT into CHON/PROT NPs depended on the concentration of CHON
379 and PROT solutions as well as their MMR (Table 1).

380 Visually opalescent or turbid dispersions containing NPs characterised by small and
381 homogenously dispersed particles were obtained for CHON/PROT MMRs of 2 and greater for all
382 CHON concentrations tested (i.e. 0.7, 1.4 and 2.1 mg/ml). A further increase in PROT
383 concentration, and thus a decrease in a CHON/PROT MMR, yielded physically unstable systems,
384 where phase separation and aggregation were observed. As indicated above, in the case of
385 CHON/PROT NPs without sCT the colloidal size of the dispersion was maintained even at lower
386 MMRs of 1.2-1.3. It was impossible to completely dissolve sCT at 1 mg/ml in the 0.7 mg/ml CHON
387 solution. A clear solution was formed either when 1 mg/ml sCT was dissolved in more
388 concentrated CHON solutions (i.e. 1.4 and 2.1 mg/ml) or when 0.5 mg/ml sCT was dissolved in
389 the 0.7 mg/ml CHON solution. Generally, the incorporation of sCT into CHON/PROT NPs resulted
390 in an increased turbidity of the dispersions (Fig. 1 and Table 1). The turbidity increased with a
391 decrease in a CHON/PROT MMR and an increase in the concentration of CHON and PROT as
392 well as the concentration of sCT.

393 The hydrodynamic diameter of the CHON/PROT/sCT NPs particles varied between 60±6 and
394 245±32 nm (Table 1). Generally, the incorporation of 0.5 or 1.0 mg/ml of sCT did not impact on
395 the particle size, but in some cases (i.e. when the CHON/PROT MMR was 2.1 and CHON
396 concentration was 0.7 or 1.4 mg/ml) loading of sCT increased the particle size compared to
397 CHON/PROT NPs without sCT (by 50 or 90 nm, respectively). Also, incorporation of 0.5 mg/ml
398 sCT resulted in a decrease in particle size of CHON/PROT MMR=6.4 NPs (0.7 mg/ml CHON) by
399 30 nm. Formulations with higher CHON/PROT MMRs (4.2-13) were generally characterised by a
400 very small particle size below or close to 100 nm, while NPs with CHON/PROT MMRs 2-3 usually

had the particle size of 150-250 nm (Table 1). sCT-loaded CHON/PROT NPs were characterised by moderate values of PDI (0.23-0.45) and a negative surface charge (Table 1).

Table 1 shows that CHON/PROT NPs had the sCT association efficiency (AE) values between 98.4 and 99.8%. AEs were slightly higher for formulations containing lower amount of PROT and higher CHON/PROT MMRs. The differences, although statistically significant, were very small (less than 1.5%). Peptide loading varied between 13.5 and 37.8%.

3.3 Colloidal behaviour of CHON/PROT/sCT NPs in various media

The size of sCT-loaded CHON/PROT MMR=6.3 NPs depended on the composition of the continuous phase (Table 2). In diluted acetate buffer (diluted AB) or diluted PBS the particle size was not different compared to that in water, however a decrease in PDI and an increase in surface charge was observed. The increase in ionic strength of both media (AB with pH=5 and PBS with pH=7.4) resulted in an increase in particle size by approximately 50 and 120 nm, respectively, in comparison to the size in water. Even in PBS the hydrodynamic diameter of the particles was not significantly different from 250 nm. The increase in the ionic strength of the media also increased the zeta potential and the NPs became more homogenously dispersed (i.e. PDI values decreased). The change in pH of the media (AB and PBS pH=5 versus pH=7.4) did not influence the properties of the NPs significantly (Table 2). The properties of NPs in serum-free medium (pH=7.4) were comparable to those in PBS. Moreover, the properties did not change within 24 hours of storage. In the acidic medium (0.07M HCl) the particle size increased significantly to 230 nm and, similarly to other media, no further change occurred within 24 hours. A decrease in pH (HCl solution) led to an increase in the zeta potential to -10 mV.

The influence of ionic strength of the properties of NPs was also examined in NaCl aqueous solutions. The particle size and zeta potential increased, while the PDI decreased, with an increase in the ionic strength of NaCl solutions.

3.4 *In vitro* release of sCT

The amount of sCT released after 24 hours into water or diluted acetate buffer from sCT-loaded

CHON/PROT MMR=6.3 NPs was below 5% (Fig. 3). In the other media (acetate buffer, PBS, diluted PBS and HCl solution) the release was greater, 4-6% of sCT was released after 1 hour and 10-12% after 2 hours, however no burst release was observed. In HCl solution and PBS 33±0.1% and 35±1.8% of the initial amount of sCT was released after 24 hours, respectively. sCT release in acetate buffer was the same at both values of pH, 5 and 7.4, and a similar behaviour was observed in PBS (data not shown).

3.5 Solid state characterisation

Two amorphous halos, centred at around 12° and 22° 2θ, were visible on each PXRD diffractograms for CHON and PROT (Fig. 4). The 22° 2θ peak of PROT was more intense than that at 12° 2θ, however intensity of the two peaks in CHON was comparable. This shows the amorphous nature of individual polyelectrolytes with the NP carriers (COM1-COM5) also being disordered. The sample COM6 (MMR=0.2, final CHON conc.=0.16 mg/ml) of the positively charged NPs showed Bragg peaks at 11.6, 20.8, 29.1, 29.7 and 31.8° 2θ. In relation to the sCT-loaded samples subjected to dissolution studies, only the NPs in water were fully amorphous and had no single sharp diffraction peaks characteristic of an ordered structure. NPs recovered from PBS, diluted PBS and HCl solution all contained two crystalline peaks, at 27.3 and 31.8° 2θ, however the presence of an amorphous halo was apparent. The sample in acetate buffer was predominantly crystalline, while that in diluted acetate buffer had a faint Bragg peak at 32.0° 2θ.

Results of DSC studies are presented in Fig. 5 and insets show tables with data evaluation. PROT and COM6 showed a single glass transition (Tg) event each, PROT at around 185 °C, while the Tg of COM6 was 10 degrees lower. CHON and COM1-COM5 showed broad endotherms of dehydration at 97 °C (CHON) or 50-59 °C (COM1-COM5) followed by an exotherm with an onset around 218-232 °C. This exotherm had notably different enthalpies, of around 138 J/g for CHON and 39-60 J/g for COM1-COM5. Thermograms of sCT-NPs after dissolution had different shapes depending on the medium used for the studies. The exotherm was still present in all of them, however its position and magnitude was dependent on the composition of the dissolution medium.

453 The onset temperatures varied between 210 and 232 °C and the peak enthalpies were between
454 4 and 30 J/g.
455 ATR-FTIR spectra of CHON, PROT and COM1 (NPs with MMR=3.1, final CHON conc=0.7 mg/ml)
456 with band assignments and principal peak positions are shown in Fig. 6. The assignment was
457 done based on studies of Chen et al., (2005); Fajardo et al., (2012); Awotwe-Otoo et al. (2012)
458 and Bonkovoski et al., (2014). In both polyions one of the most prominent vibrations is that of
459 amide I. Despite being a sodium salt, the presence of protonated –COOH moiety in CHON was
460 evident (as a shoulder at app. 1650 cm^{-1} of the amide I band and as a group at 1411 cm^{-1}).
461 Symmetric and asymmetric –S=O vibrations were also clear, however they were more intense in
462 CHON than in PROT. The spectrum of the complex had bands of both components, but position
463 and intensity of some peaks, such as those of –COOH, amide I and amide II, was different.

464 **3.6 Cytotoxicity of CHON and CHON/PROT NPs**

465 CHON even at a concentration of 5 mg/ml did not exert any toxic effects on Caco-2 cells (125±10
466 % of viable cells). PROT complexed to CHON was significantly less cytotoxic than the same
467 amount of PROT dissolved in serum-free medium (Fig. 7). The cytotoxicity of PROT has been
468 described by Umerska et al., (2014a) and its IC_{50} was found to be 0.24±0.01 mg/ml. 83±5% of
469 cells remained alive after 72 hours of exposure to CHON/PROT NPs containing 0.25 mg/ml of
470 PROT, compared to 61±10% for solution containing an equivalent content of PROT. No cytotoxic
471 effects were observed after first 1:1 v/v dilution of the NPs with the serum-free medium (98±5%
472 of viable Caco-2 cells). At this concentration (0.125 mg/ml) of PROT a significant toxic effect was
473 still observed for PROT dissolved in the medium.

474 **4. Discussion**

475 **4.1 CHON/PROT NPs: formation and formulation variables**

476 CHON/PROT NPs were spontaneously formed using mild fabrication conditions, by mixing
477 aqueous solutions of polyelectrolytes at room temperature. Similar methods were used previously
478 to obtain other polyelectrolyte complex NPs such as HA/chitosan (Umerska et al., 2012),

chondroitin/chitosan (Yeh et al., 2011, Place et al., 2014), HA/PROT (Umerska et al., 2014a) and HA/polyarginine (Oyarzun-Ampuyero et al., 2011). The process of preparation of polyelectrolyte complex NPs described above does not involve the use of cross-linkers, organic solvents or surfactants and a homogenisation step is not needed. This is an advantage over the methods commonly used to fabricate NPs of polyesters, e.g. PLGA, which require the use of organic solvents, surfactants and sometimes high temperature or homogenisation (des Rieux et al., 2006).

One of the interesting characteristics of polyelectrolytes is their ability to produce stable interpolymer complexes between oppositely charged species (Dautzenberg, 2000). CHON has multiple negative charges at physiological pH coming from sulphate and carboxyl groups. Due to the high arginine content protamines are strongly basic and have isoelectric point around 12, therefore in all pH conditions tested in this work (pH between 1.2 and 7.4) PROT has a net positive charge and can be considered as a polycation. Polyion complexation was evident by ATR-FTIR. First of all, the band at app. 1650 cm^{-1} of carbonyl moiety of CHON disappeared completely in the spectrum of complex, either due to complexation or overlap with the amide I group (Fig. 6). Amide I and II vibrations in CHON and PROT were seen to change positions indicating a change in intermolecular interactions. The band of –S=O stretching vibrations in the complex was less intense than in pure CHON, although it did not move. Electrostatic interactions between the sulphate groups of CHON and the amine moieties of chitosan were seen in the range of 1150–1300 cm^{-1} by Kaur et al. (2010) and shifts in the sulphate absorptions for carrageenan/PROT complexes were noted by Dul et.al. (2015). On the other hand, skeletal vibrational modes (–C-O-C- and -S-O-C- groups) of CHON in the complex remained in the same positions inferring that CHON and PROT interact with each other electrostatically. In summary, CHON/PROT NPs are formed by electrostatic interactions between negatively charged sulphate and carboxylate groups of CHON and positively charged amino acid residues in arginine-rich PROT molecules.

It is commonly accepted that polyelectrolyte complex formation is mainly caused by strong

505 interactions between oppositely charged polyelectrolytes, whereby the gain in entropy due to the
506 release of the low molecular counterions, initially bound to polyelectrolytes, plays a decisive part
507 (Dautzenberg and Jaeger, 2002; Schatz et al., 2004). A similar mechanism (i.e. via electrostatic
508 interactions) has already been confirmed to be responsible for formation of the complex NPs (e.g.
509 Umerska et al., 2012, 2014a and 2014b).
510 Polyelectrolyte complex dispersions may have the appearance of a solution, an opalescent or
511 turbid system or a two-phase system consisting of precipitated complex and supernatant liquid.
512 Usually, there is a narrow window of physicochemical conditions where the complexes are formed
513 and stay in the form of colloidal dispersion (de Kruif et al., 2004). The process of NP formation is
514 best conducted in diluted solutions in order to prevent macroscopic gelation, which may lead to
515 bulk hydrogels (Oh et al., 2009). In this work, the concentration of both polyelectrolytes in the final
516 dispersion was below 1% w/v (0.1-0.7% w/v). HA nanocomplexes described previously were
517 formed at comparable conditions (0.1-0.2% w/v) (Umerska et al., 2012, 2014a). It was possible
518 to obtain CHON-based NPs at higher polyanion concentrations (i.e. between 0.3 and 0.7% w/v)
519 than the HA-based NPs possibly due to the lower molecular weight of CHON (58.6 kDa) and
520 consequently lower viscosity of its solutions. It was observed however, that at a higher
521 concentration (i.e. 2.1 mg/ml or 3.6 mg/ml of CHON) the particles were markedly larger and were
522 characterised by a broader size distribution compared to lower CHON concentrations (0.7 mg/ml
523 or 1.4 mg/ml), possibly due to more frequent interparticulate interactions resulting from their
524 increased numbers.
525 When both polyions are used in equivalent net charge amounts, the particle yield is maximal
526 (Boddohi et al., 2009). On the other hand, it has been shown that, as a result of charge
527 neutralisation, aggregation of polyelectrolyte complex NPs occurs and a phase separation takes
528 place (Boddohi et al., 2009; Umerska et al., 2012). The formation of stable polyelectrolyte complex
529 NPs requires that the constituent polyelectrolyte solutions are mixed in non-stoichiometric ratios
530 (Boddohi and Kipper, 2010). The amount of CHON incorporated in NPs is presented in Figure 1S

and it is clear that the nanocomplexes are stabilised by the excess of the polyanion.

The stability of polyelectrolyte complex NPs depends on the repulsion between similarly charged particles. Consequently, the net charge of the system must be either sufficiently positive or negative if the system is to be physically stable. The polyanion/polycation MMRs, which produced phase separation, were lower for CHON/PROT systems, compared to HA/PROT polyelectrolyte complexes described previously (Umerska et al., 2014a) (polyanion/polycation MMRs of 1 and 1.4-1.6, respectively). Therefore CHON is capable of neutralising more PROT in the form of colloidal dispersion compared to HA and/or this reaction is more efficient in CHON/PROT systems. This may be due to the difference in the density of acidic sites between both molecules. CHON has a low charge density and contains residues of weak and strong acid groups present alternately every two monosaccharide, while hyaluronic acid is a weak polyacid with a charge density much lower than CHON, since only one charge can be present every two residues in HA molecules (Denuziere et al., 1996).

The particle size increased with an increasing amount of PROT in the formulation (decreasing CHON/PROT MMR) due to neutralisation of CHON by the polycation and attainment of a more compact structure of NPs. A similar tendency was observed for HA/PROT NPs (Umerska et al., 2014a). The magnitude of size of CHON/PROT NPs (between 78 and 296 nm) was similar to CHON/polyethylenimine NPs (between 92 and 207 nm) (Pathak et al., 2009) and generally smaller than CHON/chitosan NPs (between 178 and 370 nm (Yeh et al., 2011) or between 230 and 260 nm (Place et al., 2014)) or N,N,N- trimethylchitosan (between 380 and 540 nm (Place et al., 2014)). Yeh et al., (2011) also observed that at a fixed MMR (of CHON and chitosan) the particle size increased with increasing polymer concentration, which is in agreement with our observations.

Zeta potential magnitude is a surrogate marker for the colloidal stability of NPs. The charge develops as a function of the excess polymer and is controlled by an ordered polyelectrolyte complex assembly process (Hartig et al., 2007). The negative zeta potential of these NPs is similar

557 to those obtained for HA/PROT NPs (Umerska et al., 2014a). NPs with positive zeta potential had
558 very poor colloidal stability and thus were not regarded as suitable nanocarriers.
559 CHON/PROT NPs and HA/PROT NPs (Umerska et al., 2014a) differ from chitosan polyelectrolyte
560 complexes, e.g. HA/chitosan (Boddohi et al., 2009, Umerska et al., 2012), heparin/chitosan
561 (Boddohi et al., 2009) and chitosan/dextran (Schatz et al., 2004), because the hydrodynamic
562 diameter of chitosan-based NPs decreases during titration with an oppositely charged
563 polyelectrolyte, until a secondary aggregation was obtained, preceding irreversible flocculation.
564 The semi-crystalline nature of the positively charged NPs (COM6, MMR=0.2, final CHON
565 conc.=0.16 mg/ml) was surprising, considering that the starting polyelectrolyte compounds and
566 negatively charged NPs were PXRD amorphous (Fig. 4). The peak at 31.8° 2θ can possibly be
567 ascribed to sodium chloride, however the rest of Bragg peaks did not match the positions of
568 diffraction peaks of sodium sulphate, anhydrous or hydrates. Sodium sulphate is expected to be
569 formed as CHON is used as a sodium salt, while PROT as a sulphate salt. Published reports
570 indicate that polyelectrolyte complexes could be either amorphous, such as chitosan/CHON
571 (Denuziere et al., 1996), chitosan/HA (Denuziere et al., 1996), poly[(2-dimethylamino) ethyl
572 methacrylate]/CHON (Bonkovoski et al., 2014) or crystalline, for instance chitosan/quinoa protein
573 (Abugoch et al., 2011) and pectin-NH_2/CHON (Fajardo et al., 2012).
574 The thermogram of CHON (Fig. 5) was consistent with that published previously by Jo et al.
575 (2012). Bonkovoski et al. (2014) stated that CHON thermally degrades around 230 °C, thus the
576 exothermic event by DSC is of decomposition. CHON complexation to PROT resulted in a change
577 in hydration properties of the complexes, as evidenced by the shift of the peak of dehydration
578 endotherm from app. 97 °C to 50-59 °C for the negatively charged NPs and it was absent for
579 COM6 (positively charged NPs). Furthermore, COM6 had a visible Tg event, appearing at a lower
580 temperature than that of pure PROT. Complexation of PROT to CHON resulted in a significant
581 decrease of enthalpy of the exothermic transition, which can be due to the changing strength of
582 interactions in the complex. A similar observation was made by Wen et al. (2012) for dermatan

583 sulphate/alginate polyelectrolyte complexes. Nevertheless, no correlation was discerned between
584 the thermal parameters of the carriers and formulation variables such as MMR or CHON
585 concentration.
586 The poor physical stability of positively charged NPs was evident from kinetic plots (Fig. 2). As
587 previously presented, this issue with stability was also seen for HA/PROT NPs (Umerska et al.,
588 2014a) and attributed to a large difference in the molecular weight of both components (~35-fold).
589 Boddohi et al. (2009) stated that if the polyion in excess (PROT) has a much lower molecular
590 weight than the other polymer (HA in the above example), poor colloidal stability of the NPs is
591 observed. As the difference in the molecular weight of PROT and CHON is approximately 10-fold,
592 the same factor might be responsible for the physical instability of the positivity charged NPs.
593 Moreover, PXRD and DSC analyses of these NPs (COM6) indicated a semi-crystalline structure
594 of the polyelectrolyte complex formed, in contrast to the amorphous nature of the negatively
595 charged NPs. Therefore the factors compromising further the colloidal stability is the lowering of
596 surface energy and a decrease in surface area triggered by repulsion of water from the crystalline
597 segments (Caldwell et al., 2010).

598 **4.2 Formation and characterisation of sCT-loaded CHON/PROT NPs**

599 The charge of polyelectrolytes is the most important factor for their self-assembly in NPs. The
600 protein and polymers must bear opposite charge in order to form polyelectrolyte complexes
601 (Cegnar and Kerč, 2010). The results show that using high concentrations of PROT and low
602 CHON/PROT MMRs is not advised if very small NPs below 100 nm are to be obtained.
603 The high association efficiency and drug loading are in agreement with the results obtained for
604 sCT-loaded polyelectrolyte complex NPs described previously (Umerska et al., 2014a and
605 Umerska et al., 2014b). Polyelectrolyte complexes have the ability to undergo reactions of
606 polyelectrolyte substitution and exchange (Kabanov and Kabanov, 1995). Indeed, it has been
607 suggested that in ternary HA/PROT/sCT complexes the competition occurs between positively
608 charged PROT and sCT molecules for binding with negatively charged carboxylic groups of HA

609 (Umerska et al., 2014b) and the interaction between PROT and HA has been suggested to be
610 stronger than between sCT and HA. A decrease in AE values from 98 to 85% was observed when
611 the HA/PROT MMR decreased from 6 to 2 consistent with substitution of small fraction of sCT by
612 PROT. In similar conditions in CHON/PROT NPs the decrease in AE values, although statistically
613 significant ($p=0.0274$), was much smaller (99.7±0.1 and 98.7±0.5% for CHON/PROT MMRs of 6
614 and 2, respectively). Moreover, binding of sCT by CHON/PROT NPs was significantly higher than
615 by HA/PROT NPs. Also, the incorporation of sCT into HA/PROT NPs had a more pronounced
616 impact on their properties (especially the zeta potential) compared to CHON/PROT NPs. This
617 behaviour may be attributed to the higher charge density of CHON compared to HA.

618 **4.3 The influence of the dispersant on the properties of CHON/PROT/sCT NPs**

619 The properties of polyelectrolyte complex NPs depend on many parameters, also on the
620 properties of the dispersant such as its ionic strength and pH (Boddohi et al., 2009). It can be
621 expected that the properties of polyelectrolyte complexes can change depending on the medium,
622 as polyelectrolyte complexes are self-assembling objects thermodynamically stable under certain
623 conditions of medium composition, pH and ionic strength (Kabanov and Kabanov, 1995).

624 The values of zeta potential in all slightly acidic or neutral media were negative and close to -30
625 mV, therefore indicating a good colloidal stability of the NPs (Table 2). Even at acidic pH of 1.2,
626 which could be encountered e.g. in stomach, the particles maintained the negative charge. The
627 decrease of zeta potential from -47 mV in water to -10 mV in HCl solution suggests that the
628 Coulomb interactions between positively charged sCT and negatively charged CHON become
629 weaker, but are still present. Indeed, the *in vitro* release studies showed that more than 65% of
630 sCT was associated with the particles after 24 hours of incubation at acidic pH.

631 It is known that two different effects govern the behaviour of polyelectrolyte complexes after a
632 subsequent change of the ionic strength of the medium, namely secondary aggregation or
633 dissolution, depending on the nature of the components of the system (Dautzenberg, 2000). In
634 CHON/PROT NPs a significant increase in particle size was observed, especially in NaCl solution

635 and in PBS (where NaCl is the main component). This is similar to the results obtained by
636 Oyarzun-Ampuyero et al., (2009), who observed an increase in the particle size of heparin-loaded
637 chitosan/HA NPs after contact of the NPs with PBS or Hank's Balanced Salt Solution (HBSS)
638 compared to the particle size in water. However, partial dissolution was observed in PBS for
639 HA/PROT NPs described previously (Umerska et al., 2014a).
640 The interactions between oppositely charged macromolecules depend on the strength of their
641 acidic or basic groups, their charge density and the degree of neutralisation (Denuziere et al.,
642 1996). It is known that weak complexes are formed between polyelectrolytes containing weak
643 acidic and basic groups, while oppositely charged polymers containing anions and cations of
644 strong acids and bases generally form very strong polyelectrolyte complexes (Denuziere et al.,
645 1996). CHON, in contrast to HA, also contains strong acid groups (sulphates) and therefore forms
646 stronger complexes than HA. It is likely that molecules of the dispersant can penetrate the network
647 of weak nanoplexes easier. This phenomenon appears to dominate in diluted HA/PROT NPs
648 leading to their dissolution (Umerska et al., 2014a). In stronger and more compact CHON/PROT
649 complexes the dissociation of the complex as a result of screening of the charges by salt is lower
650 and the secondary aggregation predominates, which can be observed as the increase in the
651 particle size or even in the separation of the phases (Table 2).
652 Interestingly, chloride anions (present both in NaCl solution and in PBS) appeared to exert a
653 stronger effect on the properties (especially the particle size) of the CHON/PROT/sCT NPs than
654 acetate. CHON/PROT/sCT NPs dispersed in acetate buffer with the ionic strength of 0.1M were
655 characterised by significantly smaller particle size compared to NaCl solution with the ionic
656 strength of 0.075M (150 nm and 210 nm, respectively). It may be due to the fact that in the
657 Hofmeister series acetate anion is more kosmotropic compared to more chaotropic chloride anion.
658 The kosmotropes, which are able to induce order by creating hydrogen bonding throughout water,
659 are hydrated ions and exert stabilising and salting-out effects on proteins and macromolecules.
660 On the other hand, chaotrops are able to disrupt water structure, destabilise folded proteins and

give rise to salting-in behaviour (Zhang and Cremer, 2006). Alternatively, the decrease in the hydrodynamic radius of NPs induced by the acetate ions can be through a salting-out effect as the CHON chains on the exterior of NPs will find themselves in a poorer solvent, while the increase in the size caused by NaCl can be explained by a partial dissociation and/or dissolution of the polyelectrolyte complexes.

4.4 *In vitro* release of sCT

The kinetics of peptide or protein release from ionic hydrogels depends on various structural parameters of the protein and polyelectrolyte as well as on the environmental conditions inside the hydrogel (Cooper et al., 2005). The release data (Fig. 3) was fitted to the first order equation, as no burst phase was observed and confirmed when the data was fitted to the Gallagher-Corrigan model (Gallagher and Corrigan, 2000), and the parameter estimates obtained and related statistics are summarised in Table 3.

The release rate constant (k) was greatest for the NPs in the acetate buffer but the greatest amount of sCT released at infinity (W_∞) was estimated with PBS. The values of release rate constant (k) of sCT from CHON/PROT NPs were markedly lower than those of HA-based NPs (Umerska et al., 2014a) and the k parameter was approximately a 4-fold lower for CHON/PROT NPs in PBS. Therefore the peptide/NP complex is stronger in CHON-based NPs compared to HA-based NPs, which is also supported by lower amounts of sCT released from CHON/PROT NPs. This is in agreement with outcomes of studies of Kamiya and Klibanov (2003) on lysozyme release from its water-insoluble complexes.

A good linear correlation between the ionic strength of release medium, but not pH, and sCT released after 24 h (R^2=0.83, p=0.007) and the particle size of NPs in the media (R^2=0.89, p=0.003) was found. However, the release rate (k) was not found to be reliant on the ionic strength of medium. Chen et al., (2007), who examined the release of bovine serum albumin (BSA) and R6G (Rhodamine 6G) from chitosan/dextran sulphate NPs in PBS with different ionic strength also observed that the greatest release of both proteins occurred in the release media of a high

ionic strength. Sustained release of BSA and doxorubicin from CHON/chitosan polyelectrolyte NPs was reported by Yeh et al (2011) and Tsai et al. (2011), respectively, with evidence that BSA release properties were pH sensitive. Release of sCT from CHON/PROT MMR=4.2 NPs was comparable to those from CHON/PROT MMR=6.3 (data not shown), it may be concluded that release of the loaded bioactive from CHON-based NPs is influenced mainly by the peptide interactions with the polyanion (CHON) and not with the polycation.

As the sCT-loaded sample subjected to dissolution studies in water was fully amorphous and retained a majority of the loaded sCT, it can be concluded, based on PXRD and DSC data, that the peptide was molecularly dispersed within the polyelectrolyte complex. NPs recovered from PBS, diluted PBS and HCl solution had two crystalline peaks characteristic of sodium chloride. This was expected as PBS contains sodium chloride and in the HCl medium this salt can be formed from the sodium ion originating from CHON. NPs after dissolution in acetate buffer retain the buffer salts, showing as anhydrous sodium acetate (Onwudili and Williams, 2010) however, the sample from diluted acetate buffer was practically fully amorphous (with a very weak peak 32.0° 2θ of either sodium chloride or sodium acetate). Interesting information in relation to the sCT NPs was obtained from the thermal analysis studies. While the shape of the thermograms was strongly dependent on the type of medium used, the decomposition exotherm was still present in the samples (Fig. 5). Upon incorporation of the peptide, the enthalpy further decreased. Observing that the enthalpy of the exotherm changed when different dissolution media were used, an attempt was made to correlate this parameter with the amount of sCT remaining in NPs after 6h of dissolution studies. This relationship was found to be statistically significant ($p<0.008$, $R^2=0.827$) and could be described by this linear equation (Eqn. 4):

$$amount\ of\ sCT\ released\ from\ NPs\ (\mu g) = -2.65 * enthalpy\ of\ exothermic\ peak + 82.7 \quad \text{(Eqn. 4)}$$

This implies that thermal analysis can be a very useful tool when assessing the amount of actives

713 released from polyelectrolyte complexes and indeed the thermal decomposition peak might reflect
714 the strength of intermolecular interactions in such complexes. The amount of sCT not released
715 from NPs under the conditions of the *in vitro* experiment indeed remained strongly complexed to
716 CHON.

717 **4.5 Cytotoxicity of CHON and CHON/PROT NPs**

718 The cytotoxicity of CHON and NPs was examined in Caco-2 cells to assess any potential toxic
719 interactions with cells. The toxicity of the PROT in Caco-2 cells has already been reported by our
720 group (Umerska et al., 2014a). The positive charge on the cationic polymers is believed to be a
721 major cause of their cellular toxicity. These polymers were found to destabilise and ultimately
722 rupture the cell membrane as a result of strong electrostatic interaction (Pathak et al., 2009). The
723 neutralisation of PROT by the formation of nanocomplex with HA was shown to reduce the toxicity
724 of PROT (Umerska et al., 2014a). The toxic effects observed were attributed to the free PROT
725 rather that by the PROT bound to the polyanion, as the presence of low molecular weight ions in
726 the medium led to the dissociation of a subset of the HA/PROT nanocomplexes, resulting in
727 release of PROT molecules. CHON/PROT NPs appear to be less toxic than HA/PROT NPs. The
728 protective effect of polyanion in CHON/PROT NPs was observed in NPs containing 0.25 mg/ml
729 PROT, while in HA/PROT NPs the protective effect of HA was observed only at lower
730 concentration. Because CHON forms stronger electrostatic complexes with PROT than HA, the
731 amount of PROT released from CHON/PROT complexes is expected to be smaller compared to
732 HA/PROT complexes, and therefore CHON/PROT exerted less significant toxic effects.
733 Complexation to CHON has also been reported to significantly decrease the cytotoxicity of
734 polyethylenimine in HepG2 and HeLa cells (Pathak et al., 2009).

735 **5. Summary and conclusions**

736 A new type of a nanocarrier composed of CHON and PROT has been successfully developed
737 and characterised. The formation and properties of CHON/PROT NPs depended mainly on the
738 MMR of polyion components, but also on their concentration. By modulation of formulation

conditions it was possible to obtain small (100 nm and less) NPs with a narrow size distribution (PDI below 0.25). sCT was very efficiently (approximately 100%) associated with the NPs and good peptide loading (14-38%) was achieved. Some of the sCT-loaded CHON/PROT NPs were as small as 60 nm. CHON/PROT NPs were capable of providing extended release of sCT. CHON/PROT NPs maintained the negative surface charge and more than 65% of sCT was still associated with the particles after 24 hours of incubation at acidic pH values (pH=1.2). Ionic strength and composition of the medium were found to have a significant influence on the release of sCT from CHON/PROT NPs. PXRD was found to provide an insight into the solid state properties of the nanoplexes and revealed a semi-crystalline nature of the positively charged system that was linked to its poor colloidal stability. The effectiveness of thermal techniques in assessing the amount of actives released from polyelectrolyte complexes was demonstrated. As complexation to CHON markedly reduced the toxic effects exerted on cells by PROT, CHON/PROT NPs were found to be compatible and well tolerated by Caco-2 cells showing a considerable promise of these NPs in clinical applications.

6. Acknowledgments

This study was supported by the Irish Drug Delivery Research Network, a Strategic Research Cluster grant (07/SRC/B1154) under the National Development Plan co-funded by EU Structural Funds and Science Foundation Ireland and the Synthesis and Solid State Pharmaceutical Centre funded by Science Foundation Ireland under grant number 12/RC/2275. CM is SFI Stokes lecturer.

References

Abugoch, L.E., Tapia, C., Villamán, M.C., Yazdani-Pedram, M., Díaz-Dosque M., Characterization of quinoa protein–chitosan blend edible films, Food Hydrocolloids 2011; 25: 879-886.

763 American Hospital Formulary Service (AHFS) Drug Information, American Society of Hospital
764 Pharmacists Inc., Bethesda MD 1989, 1725–1736

765 Awotwe-Otoo, D., Agarabi, C., Keire, D., Lee, S., Raw, A., Yu, L., Habib, M.J., Khan, M.A., Shah,
766 R.B., Physicochemical characterization of complex drug substances: evaluation of structural
767 similarities and differences of protamine sulfate from various sources. AAPS Journal 2012; 14:
768 619-626.

769 Boateng, J., Ayensu, I. and Pawar, H., Chitosan, in Mucoadhesive Materials and Drug Delivery
770 Systems (ed V. V. Khutoryanskiy), 2014, John Wiley & Sons, Ltd, Chichester, United Kingdom.

771 Boddohi, S., Kipper, M.J., Engineering nanoassemblies of polysaccharides. Advanced Materials
772 2010; 22: 2998-3016

773 Boddohi, S., Moore, N., Johnson, P., Kipper, M., Polysaccharide-based polyelectrolyte complex
774 nanoparticles from chitosan, heparin and hyaluronan. Biomacromolecules 2009; 10: 1402-1409

775 Bonkovoski, L.C., Martins, A.F., Bellettini, I.C., Garcia, F.P., Nakamura, C.V., Rubira, A.F., Muniz,
776 E.C. Polyelectrolyte complexes of poly[(2-dimethylamino) ethyl methacrylate]/chondroitin sulfate
777 obtained at different pHs: I. Preparation, characterization, cytotoxicity and controlled release of
778 chondroitin sulphate. International Journal of Pharmaceutics 2014; 477: 197–207

779 Caldwell, M.A., Raoux, S., Wang, R.Y., Wong, P.H.-S., Milliron, D.J., Synthesis and size-
780 dependent crystallization of colloidal germanium telluride nanoparticles. Journal of Materials
781 Chemistry 2010; 20: 1285-1291

782 Cegnar, M., Kerč, J., Self-assembled polyelectrolyte nanocomplexes of alginate, chitosan and
783 ovalbumin. Acta Chimica Slovenica 2010; 57: 431-441

784 Chen, W.-B., Wang, L.-F., Chen, J.-S., Fan, S.-Y., Characterization of polyelectrolyte complexes
785 between chondroitin sulphate and chitosan in the solid state. Journal of Biomedical Materials
786 Research Part A 2005; 75:128-137

787 Chen, Y., Mohanraj, V.J., Wang, F., Benson, H.A.E., Designing chitosan-dextran sulfate
788 nanoparticles using charge ratio. AAPS PharmSciTech 2007; 8: Article 98 (E1-E9)

789 Cooper, C.L., Dubin, P.L., Kayimazer, A.B., Turksen, S., Polyelectrolyte- protein complexes.
790 Current Opinion in Colloid & Interface Science 2005; 10: 52-78

791 Corrigan, D.O., Healy, A.M., Corrigan, O.I., Preparation and release of salbutamol from chitosan
792 and chitosan co-spray dried compacts and multiparticulates. European Journal of Pharmaceutics
793 and Biopharmaceutics 2006; 62: 295-305

794 Dautzenberg, H., Light scattering studies on polyelectrolyte complexes. Macromolecular
795 Symposia 2000; 162: 1-21

796 Dautzenberg, H., Jaeger, W., Effect of charge density on the formation and salt stability of
797 polyelectrolyte complexes. Macromolecular Chemistry and Physics 2002; 203: 2095-2102

798 de Kruif, C.G., Weinbreck, F., de Vries, R., Complex coacervation of proteins and anionic
799 polysaccharides. Current opinion in Colloid & Interface Science 2004 ; 9 : 340-349

800 Denuziere, A., Ferrier, D., Domard, A., Chitosan-chondroitin sulfate and chitosan-hyaluronate
801 polyelectrolyte complexes. Physico-chemical aspects. Carbohydrate Polymers 1996; 29: 317-323

802 des Rieux, A., Fievez, V., Garinot, M., Schneider, Y.-J., Préat, V., Nanoparticles as potential oral
803 delivery systems of proteins and vaccines: A mechanistic approach. Journal of Controlled
804 Release 2006; 116: 1-27

805 Dul, M., Paluch, K.J., Kelly, H., Healy, A.M., Sasse, A., Tajber, L. Self-assembled
806 carrageenan/protamine polyelectrolyte nanoplexes-Investigation of critical parameters governing
807 their formation and characteristics. Carbohydrate Polymers, 2015; 123: 339-349

808 EMA website, EMEA/H/A-31/1291, Questions and answers on the review of calcitonin-
809 containing medicines.

http://www.ema.europa.eu/docs/en_GB/document_library/Referrals_document/Calcitonin_31/WC500130149.pdf, accessed on 7th December 2014

Fajardo, A.R, Lopes, L.C., Pereira, A.G.B., Rubira, A.F., Muniz, E.C., Polyelectrolyte complexes based on pectin–NH_2 and chondroitin sulphate. Carbohydrate Polymers, 2012; 87: 1950-1955.

Gallagher, K.M., Corrigan, O.I., Mechanistic aspects of the release of levamisole hydrochloride from biodegradable polymers, Journal of Controlled Release 2000; 69: 261-272

González Ferreiro, M., Tillman, L., Hardee, G., Bodmeier, R., Characterization of complexes of an antisense oligonucleotide with protamine and poly-L-lysine salts. Journal of Controlled Release 2001; 73: 381-390

Hamidi, M., Azadi, A., Rafiei, P., Hydrogel nanoparticles in drug delivery. Advanced Drug Delivery Reviews 2008; 60: 1638-1649

Hartig, S.M., Greene, R.R., Dikov, M.M., Prokop, A., Davidson, J.M., Multifunctional nanoparticulate polyelectrolyte complexes. Pharmaceutical Research 2007; 24: 2353-2369

Jo, S., Kim, S., Noh, I., Synthesis of In situ chondroitin sulfate hydrogel through phosphine-mediated Michael type addition reaction. Macromolecular Research 2012; 20: 968-976

Junghans, M., Kreuter, J., Zimmer, A., Antisense delivery using protamine-oligonucleotide particles. Nucleic Acids Research 2000; 28(10) e45

Kabanov, A.V., Kabanov, V.A., DNA Complexes with Polycations for the Delivery of Genetic Material into Cells. Bioconjugate Chemistry 1995; 6: 7-20

Kamiya, N., Klibanov, A.M., Controlling the rate of protein release from polyelectrolyte complexes. Biotechnology and Bioengineering 2003; 82: 590-594

Kaur, G., Rana, V., Jain, S., Tiwary, A.K. Colon delivery of budesonide: evaluation of chitosan-chondroitin sulfate interpolymer complex. AAPS PharmSciTech 2010; 11: 36-45

833 Lee, Y.H., Sinko, P.J., Oral delivery of salmon calcitonin. Advanced Drug Delivery Reviews 2000;
834 42: 225-238

835 Manicourt, D.-H., Devogelaer. J.-P., Azria, M., Silverman, S., Rationale for the potential use of
836 calcitonin in osteoarthritis. Journal of Musculosceletal Neuronal Interactions 2005; 5:285-293

837 Mori, Y., Nakamura, S., Kishimoto, S., Kawakami, M., Suzuki, S., Matsui, T., Ishihara, M.,
838 Preparation and characterization of low-molecular-weight heparin/protamine nanoparticles
839 (LMW-H/P NPs) as FGF-2 carrier. International Journal of Nanomedicine 2010; 5: 147-155

840 Oh, J.K., Lee, D.I., Park, J.M., biopolymer-based microgels/nanogels for drug delivey
841 applications. Progress in Polymer Science 2009; 34: 1261-1282

842 Onwudili, J.A, Williams, P.T., Hydrothermal reactions of sodium formate and sodium acetate as
843 model intermediate products of the sodium hydroxide-promoted hydrothermal gasification of
844 biomass. Green Chemistry 2010; 12: 2214-2224

845 Oyarzun-Ampuero, F.A, Brea, J., Loza, M.I., Torres, D., Alonso, M.J., Chitosan-hyaluronic acid
846 nanoparticles loaded with heparin for the treatment of asthma. International Journal of
847 Pharmaceutics 2009; 381: 122-129

848 Oyarzun-Ampuero, F.A., Goycoolea, F.M., Torres, D., Alonso, M.J., A new drug nanocarrier
849 consisting of polyarginine and hyaluronic acid. European Journal of Pharmaceutics and
850 Biopharmaceutics 2011; 79: 54-57

851 Ozoran, K., Yildirim, M., Önder, M., Sivas, F., Inanir, A., The bone mineral density effects of
852 calcitonin and alendronate combined therapy in patients with rheumatoid arthritis. APLAR Journal
853 of Rheumatology 2007; 10: 17-22

854 Paluch, K.J., Tajber, L., McCabe, T., O'Brien, J.E., Corrigan, O.I., Healy, A.M., Preparation and
855 solid state characterisation of chlorothiazide sodium intermolecular self-assembly suprastructure.
856 European Journal of Pharmaceutical Sciences 2010; 41:603-611

857 Paluch, K.J., McCabe, T., Müller-Bunz, H., Corrigan, O.I., Healy, A.M., Tajber, L. Formation and
858 physicochemical properties of crystalline and amorphous salts with different stoichiometries
859 formed between ciprofloxacin and succinic acid. Molecular Pharmaceutics 2013; 10: 3640-3654

860 Pathak, A., Kumar, P., Chuttani, K., Jain, S., Mishra, A., Vyas, S.P., Gupta, K.C., Gene
861 expression, biodistribution and pharmacoscintigraphic evaluation of chondroitin sulphate-PEI
862 nanoconstructs mediated tumor gene therapy. ACS Nano 2009; 3: 1493-1505

863 Place, L.W., Sekyi, M., Kipper, M.J., Aggrecan-mimetic, glycosaminoglycan-containing
864 nanoparticles for growth factor stabilization and delivery. Biomacromolecules 2014; 15: 680-689

865 Reynolds, F., Weissleder, R., Josephson, L., Protamine as an efficient membrane-translocating
866 peptide. Bioconjugate Chemistry 2005; 16: 1240-1245

867 Sakuma, S., Sudo, R., Suzuki, N., Kikuchi, H., Akashi, M., Hayashi, M., Mucoadhesion of
868 polystyrene nanoparticles having surface hydrophilic polymeric chains in the gastrointestinal tract.
869 International Journal of Pharmaceutics 1999; 177: 161–172

870 Sakuma, S., Suzuki, N., Sudo, R., Hiwatari, K., Kishida, A., Akashi, M. Optimized chemical
871 structure of nanoparticles as carriers for oral delivery of salmon calcitonin. International Journal
872 of Pharmaceutics 2002; 239: 185–195

873 Schatz, C., Lucas, J.-M., Viton, C., Domard, A., Pichot, C., Delair, T., Formation and properties
874 of positively charged colloids based on polyelectrolyte complexes of biopolymers. Langmuir 2004;
875 20: 7766-7778

876 Soppimath, K.S., Aminabhavi, T.M., Kulkarni, A.R., Rudzinski, W.E., Biodegradable polymeric
877 nanoparticles as drug delivery devices. Journal of Controlled Release 2001; 70: 1-20

878 Sundar, S., Kundu, J., Kundu, S.C., Biopolymeric nanoparticles. Science and Technology for
879 Advanced Materials 2011; 11/ 014104 (13pp)

880 Torres-Lugo, M., Peppas N.A., Molecular design and in vitro studies of novel pH-sensitive
881 hydrogels for the oral delivery of calcitonin. Macromolecules 1999; 32: 6646–6651

882 Tsai, H.Y., Chiu, C.C., Lin, P.C., Chen, S.H., Huang, S.J., Wang, L.F., Antitumor efficacy of
883 doxorubicin released from crosslinked nanoparticulate chondroitin sulfate/chitosan polyelectrolyte
884 complexes. Macromolecular Bioscience 2011; 11: 680-688

885 Umerska, A., Paluch, K.J., Inkielewicz-Stępniak, I., Santos-Martinez, M.J., Corrigan, O.I., Medina,
886 C., Tajber, L., Exploring the assembly process and properties of novel crosslinker-free
887 hyaluronate-based polyelectrolyte complex nanocarriers. International Journal of Pharmaceutics
888 2012; 436: 75-87

889 Umerska, A., Paluch, K.J., Santos-Martinez, M.-J., Corrigan, O.I., Medina, C., Tajber, L., Self-
890 assembled hyaluronate/protamine polyelectrolyte nanoplexes: Synthesis, stability,
891 biocompatibility and potential use as peptide carriers. Journal of Biomedical Nanotechnology
892 2014a; 10: 3658-3673

893 Umerska, A., Corrigan, O.I., Tajber, L., Intermolecular interactions between salmon calcitonin,
894 hyaluronate and chitosan and their impact on the process of formation and properties of peptide-
895 loaded nanoparticles. International Journal of Pharmaceutics 2014b; 477, 102–112

896 van Damme, M.-P. I., Moss, J.M., Murphy, W.H., Preston, B.N., Binding properties of
897 glycosaminoglycans to lysozyme- effect of salt and molecular weight. Archives of Biochemistry
898 and Biophysics 1994; 310: 16-24

899 Volpi, N., Oral bioavailability of chondroitin sulfate (Condrosulf®) and its constituents in healthy
900 men volunteers. Osteoarthritis and Cartilage 2002; 10: 768-777

901 Wen, Y., Grøndahl, L., Gallego, M.R., Jorgensen, L., Møller, E.H., Nielsen, H.M. Delivery of
902 dermatan sulfate from polyelectrolyte complex-containing alginate composite microspheres for
903 tissue regeneration. Biomacromolecules 2012; 13: 905-917

904 Yeh, M.-K., Cheng. K.-M., Hu, C.S., Huang, Y.-H., Yong, J.-J., Novel protein-loaded chondrotin
905 sulfate-chitosan nanoparticles: Preparation and characterization. Acta Biomaterialia 2011; 7:
906 3804-3812

907 Zhang, Y, Cremer, P.S., Interactions between macromolecules and ions: the Hofmeister series.
908 Current Opinion in Chemical Biology 2006; 10: 658-663

Table 1. Composition and properties association efficiency (AE) and sCT loading of sCT-loaded CHON/PROT formulations tested. TR - transmittance, MPS – mean particle size, PDI - polydispersity index, ZP -zeta potential.

Initial CHON conc. (mg/ml)	CHON/ PROT MMR	CHON incorporated in NPs (%)	Initial sCT conc. (mg/ml)	TR (%)	MPS (nm)	PDI	ZP (mV)	AE (%)	sCT loading (%)
0.7	2.1	89±8	0.5	71±5	144±10	0.42±0.16	-32.6±3.7	98.7±0.5	32.0±0.15
0.7	6.4	73±5	0.5	97±2	60±6	0.42±0.03	-42.5±3.8	99.7±0.1	37.8±0.04
1.4	2.1	92±4	0.5	43±1	195±14	0.35±0.09	-40.0±3.9	98.8±0.3	18.9±0.06
1.4	4.2	83±3	0.5	92±1	87±6	0.35±0.07	-42.6±12.6	99.6±0.1	22.0±0.02
1.4	13.0	72±4	0.5	98±1	76±14	0.45±0.04	-44.9±11.8	99.8±0.1	24.5±0.02
1.4	2.1	95±2	1.0	22±9	168±10	0.27±0.03	-31.3±1.8	98.4±0.3	31.7±0.08
1.4	4.2	85±4	1.0	83±6	87±4	0.23±0.01	-37.7±1.0	99.5±0.1	36.0±0.03
2.1	2.1	95±2	0.5	15±3	224±13	0.30±0.01	-46.6±1.3	98.7±0.3	13.5±0.03
2.1	3.1	90±3	0.5	68±2	154±5	0.29±0.01	-48.6±7.2	99.6±0.1	15.0±0.02
2.1	6.3	83±3	0.5	92±1	95±7	0.30±0.02	-47.0±9.2	99.8±0.1	16.8±0.02
2.1	2.1	95±3	1.0	8±1	245±32	0.45±0.18	-39.6±2.5	98.4±0.1	23.7±0.02
2.1	3.1	91±2	1.0	48±7	161±12	0.28±0.01	-43.2±2.3	99.5±0.1	26.0±0.02
2.1	6.3	83±3	1.0	85±2	100±9	0.24±0.01	-47.3±5.2	99.7±0.1	28.7±0.02

Table 2. Properties of sCT-loaded CHON/PROT NPs (CHON conc. 2.1 mg/ml, sCT conc. 1 mg/ml, CHON/PROT MMR=6.3): mean particle size (MPS), polydispersity index (PDI) and zeta potential (ZP) in different media. The samples were prepared as described in Section 2.4.2 and measured after 1 hour of incubation at 37 °C. AB - acetate buffer, PBS - phosphate buffer saline, HCl - hydrochloric acid solution pH=1.2, MEM - Eagle's Minimal Essential Medium.

Medium	MPS (nm)	PDI	ZP (mV)
Water	100±9	0.24±0.01	-47.3±5.2
PBS, pH=7.4	219±17	0.09±0.04	-24.3±4.1
PBS, pH=5	213±11	0.08±0.01	-22.5±1.8
PBS, pH=7.4; 1:10 dil.	116±11	0.16±0.02	-33.7±2.2
AB, pH=5	149±13	0.06±0.03	-29.0±1.0
AB, pH=7.4	142±9	0.10±0.03	-27.8±1.5
AB, pH=5; 1:10 dil.	102±11	0.14±0.05	-32.9±5.1
HCl, pH=1.2	229±26	0.10±0.05	-10.2±1.1
MEM, pH=7.4	222±7	0.06±0.03	-24.4±1.5
1.8% NaCl	295±6	0.08±0.02	-19.8±1.2
0.9% NaCl	242±9	0.08±0.02	-18.4±1.5
0.45% NaCl	210±5	0.10±0.02	-23.1±2.1
0.23% NaCl	172±5	0.17±0.04	-22.8±2.3
0.09% NaCl	111±6	0.18±0.04	-28.9±1.5

Table 3. Model parameter estimates for sCT release data fitted to the first-order model (Eqn. 3, Section 2.4.2), where W_∞ is the amount of sCT released at infinity and k is the release rate constant. The composition of the media is shown in Section 2.4.2. AB - acetate buffer, PBS - phosphate buffer saline, IS – ionic strength.

Medium	k (h^{-1})	W_∞ (µg/mg of NPs)	Goodness of fit (R^2)
Water, IS=0.000	0.124±0.054	12.6±4.6	0.9859
HCl, pH=1.2, IS=0.070	0.221±0.011	94.4±0.8	0.9965
AB, pH=5, IS=0.070	0.389±0.012	54.3±11.6	0.9962
AB, pH=5; 1:10 dil., IS=0.007	0.088±0.105	11.6±5.3	0.9972
PBS, pH=7.4, IS=0.140	0.201±0.030	100.2±3.7	0.9961
PBS, pH=7.4; 1:10 dil., IS=0.014	0.250±0.001	72.9±0.8	0.9908

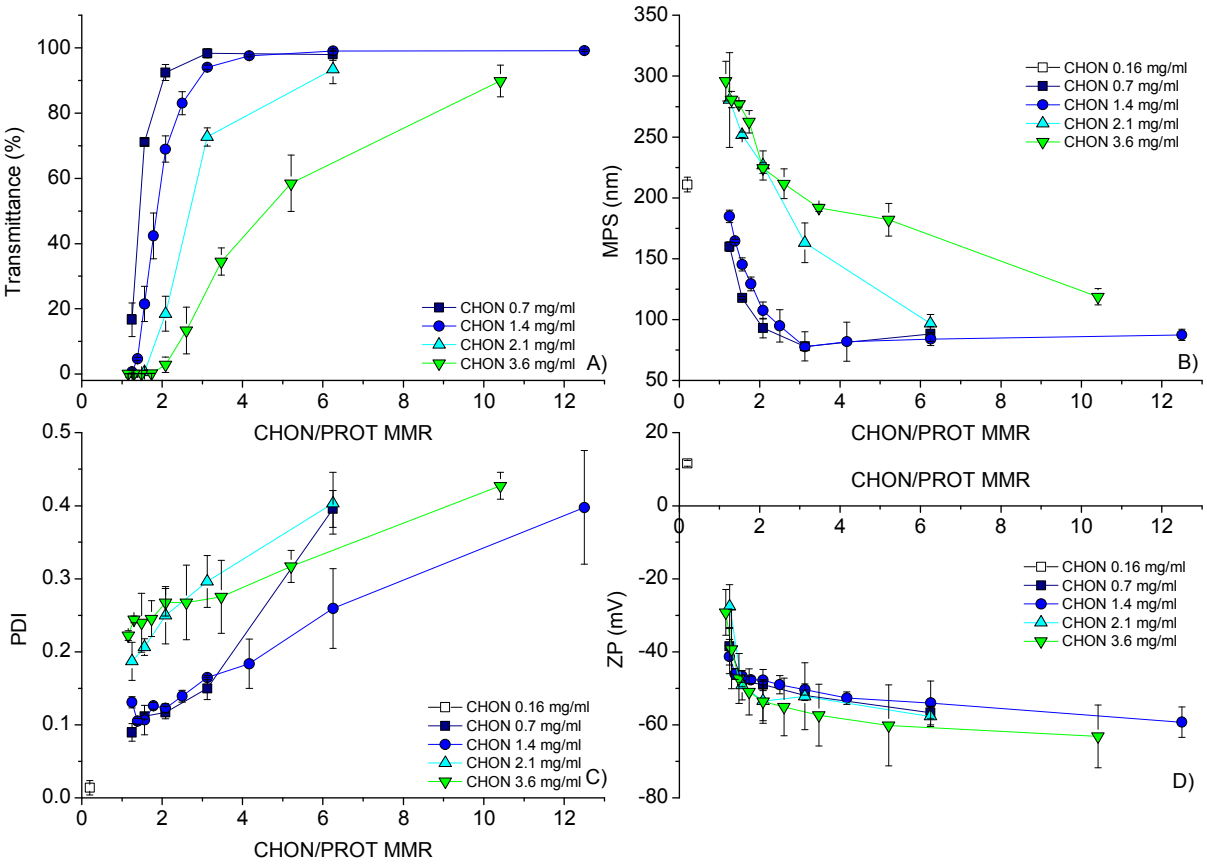

Figure 1. Properties of CHON/PROT NPs: A) transmittance, B) mean particle size (MPS), C) polydispersity index (PDI) and D) zeta potential (ZP). Conditions of analyses are presented in Sections 2.3.1 and 2.3.3. Lines are for visual guide only.

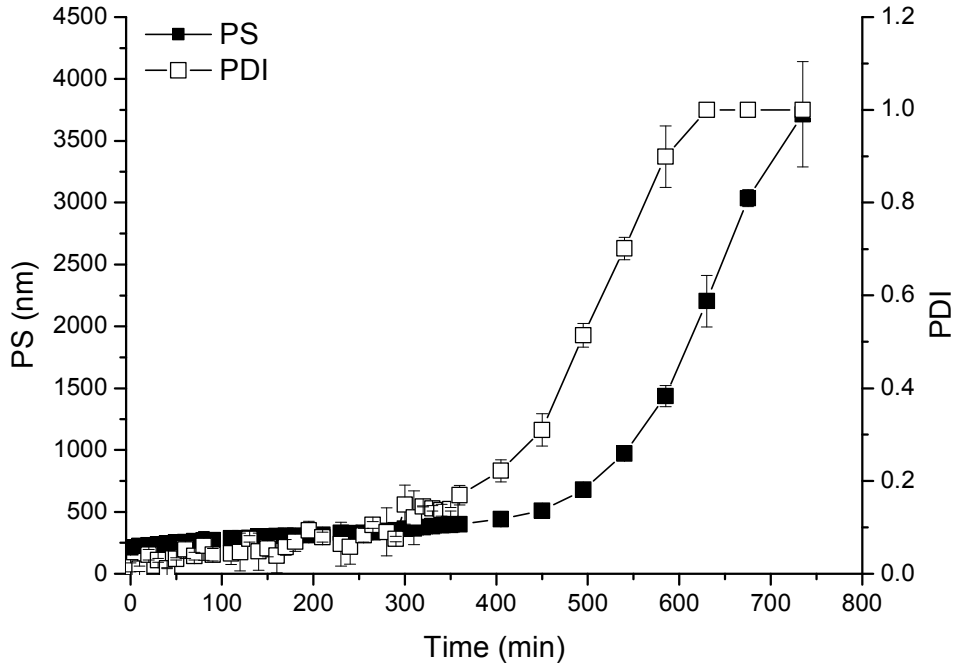

Figure 2. Kinetics of change in particle size (PS, filled squares) and polydispersity index (PDI, empty squares) of positively charged CHON/PROT NPs (PROT of 0.7 mg/ml, CHON of 0.16 mg/ml).

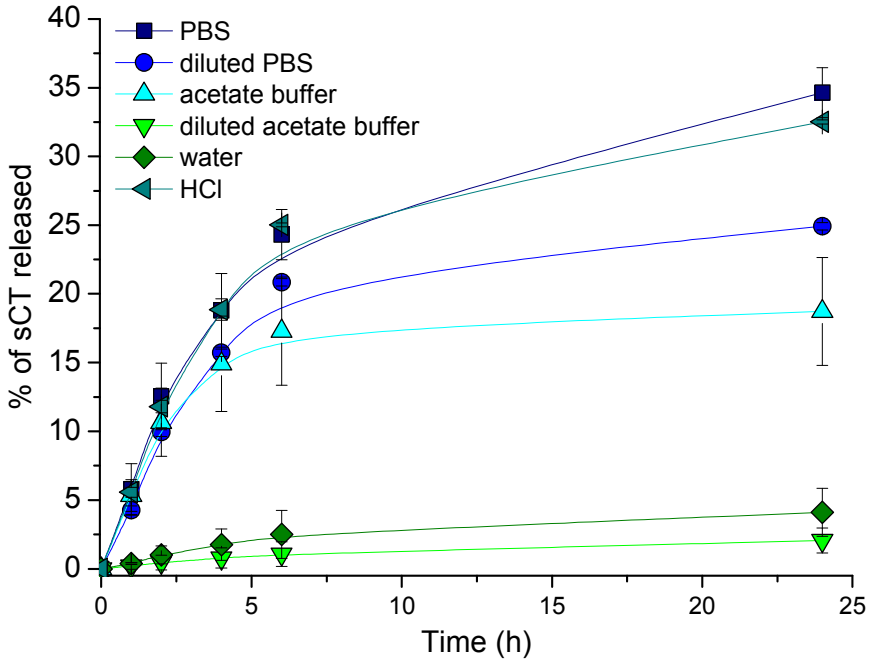

Figure 3. Cumulative release profiles of sCT from sCT-loaded CHON/PROT NPs (CHON conc. 2.1 mg/ml, sCT conc. 1 mg/ml, CHON/PROT MMR=6.3) into different media. The experiments were carried out at 37 °C. The composition of the media is shown in Section 2.4.2.

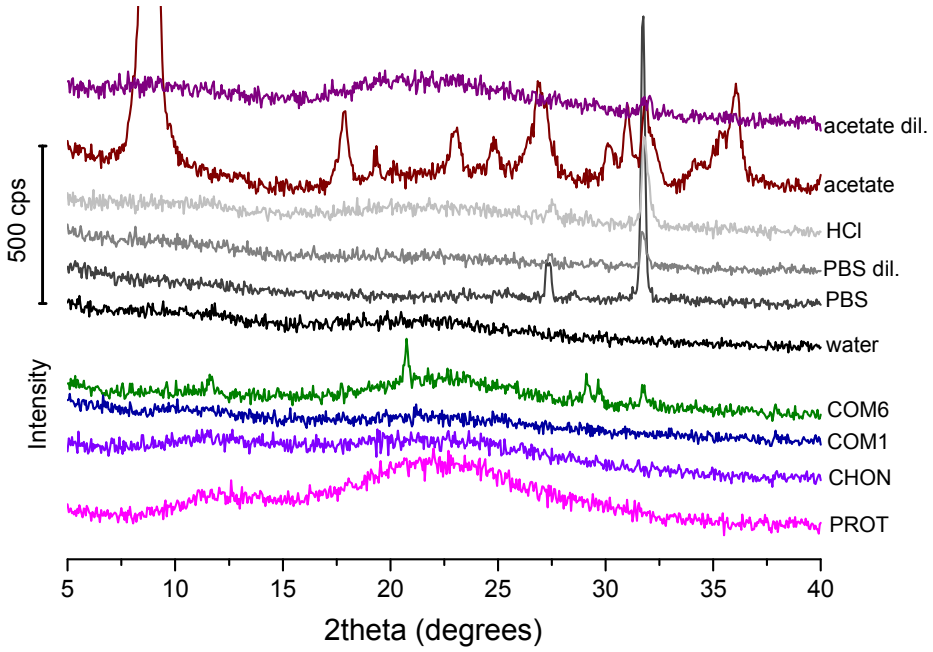

Figure 4. PXRD patterns of CHON, PROT, CHON/PROT NPs (COM1: MMR=3.1, final CHON conc.=0.7 mg/ml; COM6: MMR=0.2, final CHON conc.=0.16 mg/ml) as well as sCT-loaded NPs (CHON conc. 2.1 mg/ml, sCT conc. 1 mg/ml, CHON/PROT MMR=6.3) recovered after 6h of dissolution studies in various media: deionised water, PBS pH=7.4, diluted (1:10 v/v) PBS, HCl sol. pH=2, acetate buffer pH=5 and diluted (1:10 v/v) acetate buffer pH=5.

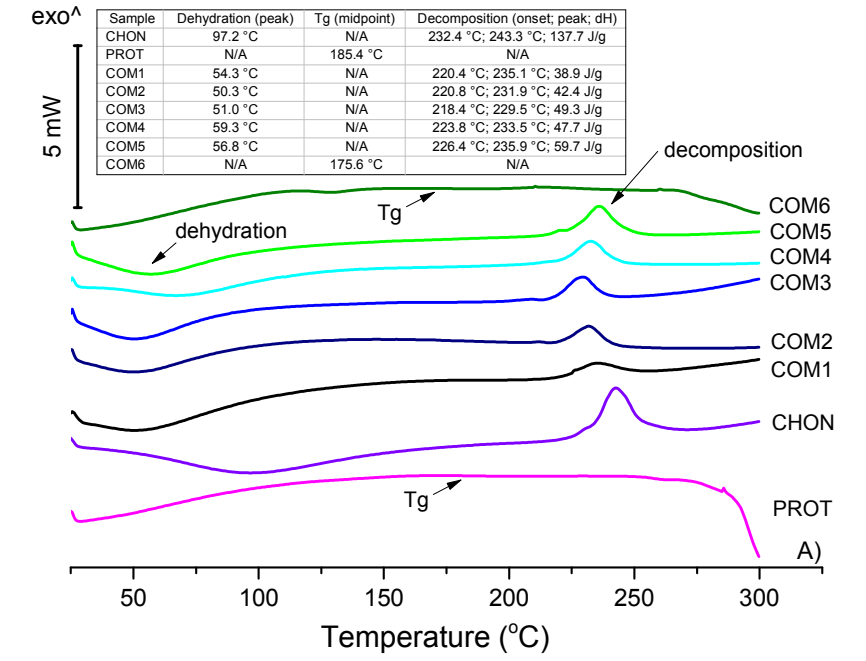

Sample	Dehydration (peak)	Tg (midpoint)	Decomposition (onset; peak; dH)
CHON	97.2 °C	N/A	232.4 °C; 243.3 °C; 137.7 J/g
PROT	N/A	185.4 °C	N/A
COM1	54.3 °C	N/A	220.4 °C; 235.1 °C; 38.9 J/g
COM2	50.3 °C	N/A	220.8 °C; 231.9 °C; 42.4 J/g
COM3	51.0 °C	N/A	218.4 °C; 229.5 °C; 49.3 J/g
COM4	59.3 °C	N/A	223.8 °C; 233.5 °C; 47.7 J/g
COM5	56.8 °C	N/A	226.4 °C; 235.9 °C; 59.7 J/g
COM6	N/A	175.6 °C	N/A

19

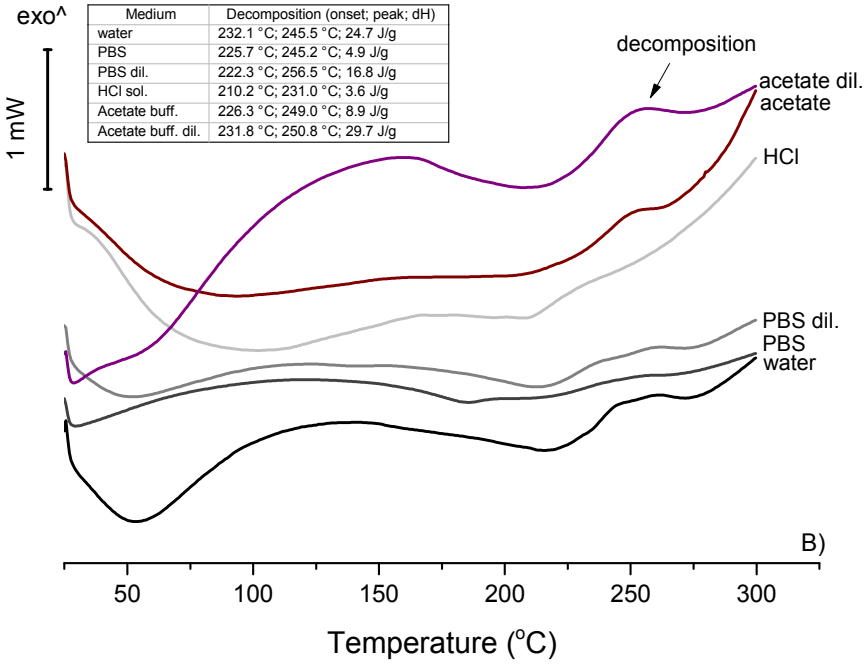

Medium	Decomposition (onset; peak; dH)
water	232.1 °C; 245.5 °C; 24.7 J/g
PBS	225.7 °C; 245.2 °C; 4.9 J/g
PBS dil.	222.3 °C; 256.5 °C; 16.8 J/g
HCl sol.	210.2 °C; 231.0 °C; 3.6 J/g
Acetate buff.	226.3 °C; 249.0 °C; 8.9 J/g
Acetate buff. dil.	231.8 °C; 250.8 °C; 29.7 J/g

20

21 Figure 5. DSC thermograms of A): CHON, PROT and CHON/PROT NPs (COM1: MMR=3.1, final
22 CHON conc.=0.7 mg/ml; COM2: MMR=3.1, final CHON conc.=1.4 mg/ml; COM3: MMR=12.5,
23 final CHON conc.=1.4 mg/ml; COM4: MMR=3.1, final CHON conc.=2.1 mg/ml; COM5: MMR=5,
24 final CHON conc.=3.6 mg/ml; COM6: MMR=0.2, final CHON conc.=0.16 mg/ml), B) sCT-loaded
25 NPs (CHON conc. 2.1 mg/ml, sCT conc. 1 mg/ml, CHON/PROT MMR=6.3) recovered after 6h of

dissolution studies in various media: deionised water, PBS pH=7.4, diluted (1:10 v/v) PBS, HCl sol. pH=2, acetate buffer pH=5 and diluted (1:10 v/v) acetate buffer pH=5. Tables present data evaluation: Tg - glass transition, dH – enthalpy of process.

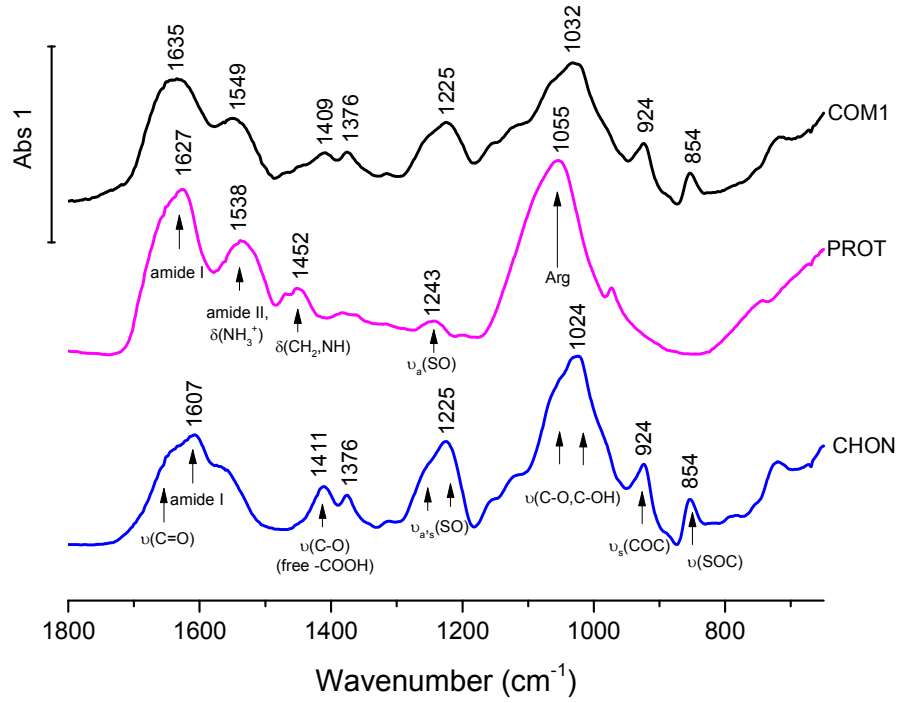

29

30 Figure 6. FTIR analysis of CHON, PROT and COM1 (NPs with MMR=3.1, final CHON conc.=0.7

31 mg/ml). v – stretching, $v_{s,a}$ – symmetric and asymmetric stretching, v_s – symmetric stretching, v_a –

32 asymmetric stretching and δ – bending vibrations. Arg – arginine. Numbers above peaks indicate

33 the position of principal bands.

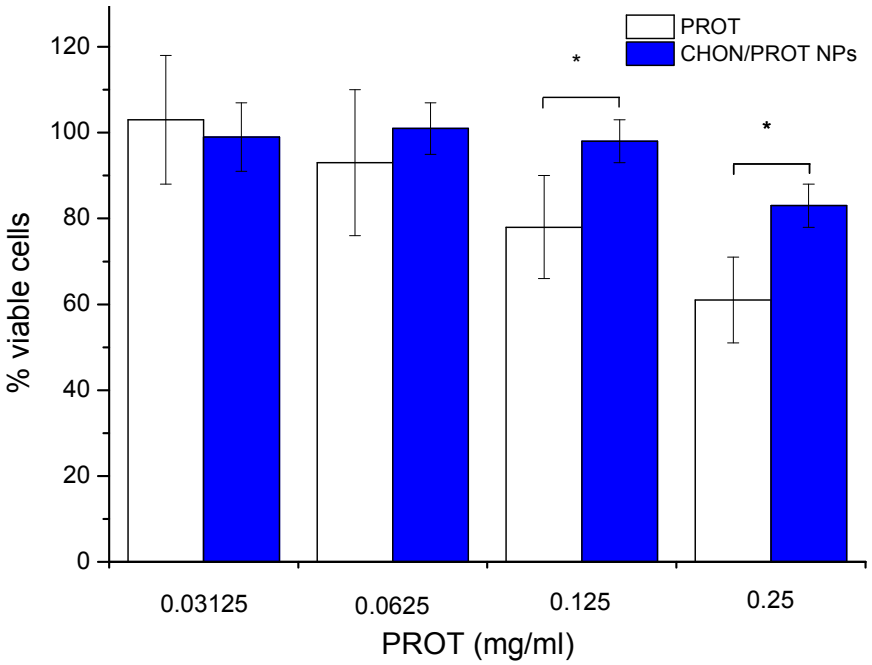

Figure 7. Viability of Caco-2 cells as measured by MTS assay after 72 h of exposure to CHON/PROT NPs (CHON/PROT MMR=3.1) and PROT (mean ± S.D., n=3). Statistical analysis: *p<0.05.